PAPER • **OPEN ACCESS**

Masonry Vaults Subjected To Horizontal Loads: Experimental and Numerical Investigations to Evaluate the Effectiveness of A GFRM Reinforcement

To cite this article: Natalino Gattesco and Ingrid Boem 2017 *IOP Conf. Ser.: Mater. Sci. Eng.* **245** 022075

View the article online for updates and enhancements.

Related content

- Jobs masonry in LHCb with elastic Grid Jobs
F Stagni and Ph Charpentier
- Influence of Grid Reinforcement Placed In Masonry Bed Joints on Its Flexural Strength
Adam Piekarczyk
- Experimental and numerical investigations on adhesively bonded joints
R Negru, L Marsavina and M Hluscu

This content was downloaded from IP address 87.4.8.214 on 18/11/2017 at 17:27

IOP Conf. Series: Materials Science and Engineering **245** (2017) 022075 doi:10.1088/1757-899X/245/2/022075

Masonry Vaults Subjected To Horizontal Loads: Experimental and Numerical Investigations to Evaluate the Effectiveness of A GFRM Reinforcement

Natalino Gattesco [1], Ingrid Boem [1]

[1] Department of Engineering and Architecture, University of Trieste, p.le Europa 1, 34127, Trieste (Italy)

boem@dicar.units.it

Abstract. The paper investigates the effectiveness of a modern reinforcement technique based on a Glass Fiber-Reinforced Mortar (GFRM) for the enhancement of the performances of existing masonry vaults subjected to horizontal seismic actions. In fact, the authors recently evidenced, through numerical simulations, that the typical simplified loading patterns generally adopted in the literature for the experimental tests, based on concentrated vertical loads at 1/4 of the span, are not reliable for such a purpose, due to an unrealistic stress distribution. Thus, experimental quasi-static cyclic tests on full-scale masonry vaults based on a specific setup, designed to apply a horizontal load pattern proportional to the mass, were performed. Three samples were tested: an unreinforced vault, a vault reinforced at the extrados and a vault reinforced at the intrados. The experimental results demonstrated the technique effectiveness in both strength and ductility. Moreover, numerical simulations were performed by adopting a simplified FE, smear-crack model, evidencing the good reliability of the prediction by comparison with the experimental results.

1. Introduction

In ancient masonry buildings of European cities, the presence of vaults supporting only their own weight (shelters) is quite common. These structural elements typically present good strength reserves against vertical loads but a very low resistance when subjected to horizontal actions, and require, thus, specific strengthening interventions so to prevent possible brittle failures during earthquakes. Modern reinforcement solutions, based on composite materials, were introduced in the last two decades, with the aim to comply both effectiveness and compatibility needs [1]-[4]. In particular, strengthening techniques based on the application of fibre-reinforced polymers (FRP), made up of synthetic or natural fibers (carbon, glass, aramid, basalt…) embedded in an inorganic matrix (fibre-reinforced cementitious matrix - FRCM - and fibre-reinforced mortars - FRM), applied to the vaults intrados or extrados, have been recently proposed and investigated [5]-[8].

The paper focuses on a compatible FRM strengthening technique consisting in the application of a reinforcement made of Glass Fibre-Reinforced Polymer (GFRP) meshes embedded in a thin mortar layer (about 30 mm), anchored to the masonry vault by means of GFRP connectors. Experimental in-plane and out-of-plane tests, performed by the authors, proved the effectiveness of the technique in strengthening existing masonry walls [9]-[10]. Moreover, a preliminary numerical study on the effectiveness of the technique in enhancing masonry vaults subjected to vertical and horizontal loads

Content from this work may be used under the terms of the Creative Commons Attribution 3.0 licence. Any further distribution of this work must maintain attribution to the author(s) and the title of the work, journal citation and DOI.
Published under licence by IOP Publishing Ltd

was carried out [11] on the basis of a FE Model developed for masonry walls subjected to out-of-plane bending [10]. The results showed the potential, excellent benefits of the reinforcement in terms of both strength and ductility. Moreover, it emerged that the typical simplified loading patterns used in the literature for the experimental tests on masonry vaults, based on concentrated vertical loads at 1/4 of the span, are not able to reproduce the actual behavior and the effectiveness of the reinforced elements subjected to horizontal seismic actions.

Thus, the authors carried out an experimental campaign on full-scale solid brick masonry barrel vaults aimed to evaluate the actual effectiveness of the technique and to validate the numerical findings. A specific rig was designed, so to reproduce the pattern of a transversal horizontal load proportional to the vault self-weight able to represent, through quasi-static cyclic tests, the stress due to horizontal seismic excitation. In particular, the paper reports and discuss the results of the first three experimental tests performed: one unreinforced vault, a vault reinforced at extrados and a vault reinforced at intrados. The three configurations are also analysed numerically, by using the FE model mentioned above, and the results are compared with the experimental ones, to evaluate the reliability of the predictions.

2. Experimental tests

The sections sums up the samples characteristics, the setup and the main results of the experimental tests performed on masonry vaults.

Sample characteristics. The experimental tests concerned three masonry barrel vaults with solid brick units arranged in a running bond normal to the vault surface (thickness 120 mm); the vaults had a width of 770 mm, a span of 4000 mm and a rise/radius ratio of 0.75 (Figure 1a). The reinforcement consisted in a 30 mm thick mortar layer with 66x66 mm^2 GFRP meshes embedded; L-shaped GFRP connectors (6 per square meter, 7x10 mm^2 cross section) were applied by insertion into holes in masonry and injection of thixotropic epoxy resin (Figure 1b).

One sample was reinforced at extrados (V02-75-RE) and one at intrados (V03-75-RI); a third unreinforced specimen (V01-75-NR) was also tested, for comparison.

The normalized compressive strength of the solid bricks resulted equal to 15.7 MPa [12]; an hydraulic lime mortar (320 kg of binder per m^3 of mortar) was adopted for the masonry: the average compressive strength was 2.93 MPa [13], the tensile strength 0.4 MPa [14]. The average thickness of the mortar joints was 10 mm.

A premixed hydraulic lime and cement mortar was used for the GFRM layers. Experimental tests evidenced a tensile strength 1.10 MPa [14] and an average compressive strength of 6.90 MPa [13]. The Young modulus, deduced from testing cylindrical samples, resulted of about 14.4 GPa [15].

The wires of the GFRP mesh (Table 1) had a 3.8 mm^2 fiber area and are coated with a thermo-hardening resin (vinyl ester epoxy and benzoyl peroxide as catalyst). The mesh was formed by weaving twisting fibers wires (wrap) across the parallel fibers ones (weft). The orientation of twisted fibers wires in vault samples followed the arch direction. The GFRP L-shaped connectors had a fiber cross section equal to 57.6 mm^2.

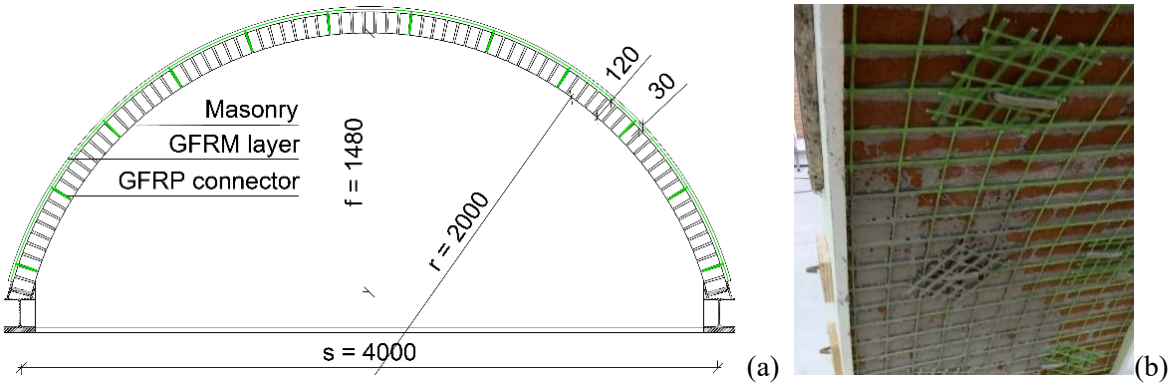

Figure 1. Main characteristics of specimens (a) and detail of application of the reinforcement at the vault intrados (b)

Table 1. Characteristics of GFRP wires or connectors: A_{tot} wire cross section, A_{fib} fiber area, T tensile resistance and EA axial stiffness.

GFRP element	A_{tot} [mm^2]	A_{fib} [mm^2]	T [kN]	EA [kN]
Parallel fiber wire	9.41	3.80	5.62	296
Twisted fiber wire	7.29	3.80	4.49	264
Connector	70.0	57.6	36.01	-

Experimental characterization tests on GFRM layers (900x132x30 mm^3) were performed to evaluate the global tensile behavior of the reinforcement (Figure 2a). The test setup and results were described in detail and discussed by the authors in [16]. The curves of the tensile stress σ against the strain ε are illustrated in Figure 2b: a first, elastic branch was detected, with stiffness dependent on the Young modulus of the mortar; then, when the mortar tensile strength was exceeded, a first transversal crack formed, resulting in a sudden decrease of the load, and then increased again. When the tensile strength of the mortar is reached once more, a new crack is formed: several cracks (spaced about 130-150 mm) gradually appeared in the mortar, located, for the most, in correspondence of transversal mesh wires. Then, the material behaves approximately linearly, with a slope almost parallel to that of the GFRP mesh alone. It is evidenced that the uncracked mortar among the cracks induced a stiffening of the behavior of the layer in respect to that of the reinforcement only. The collapse was attained when the tensile rupture of the longitudinal GFRP wires occurred.

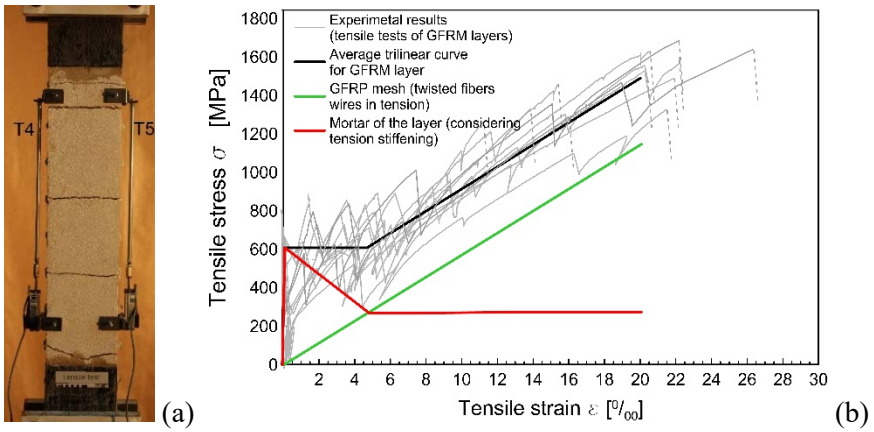

Figure 2. Tensile tests on GFRM layers: (a) test setup and (b) tensile stress σ vs. strain ε curves (tension referred to the dry area of fibers)

Test setup. The experimental apparatus (Figure 3) was composed of two robust steel frames connected through some steel transverse elements. Two hollow-piston cylinders (24 kN ± 60 mm stroke), acting horizontally and oriented in the same direction, are applied in the middle of two of these transverse elements, at opposite sides of the apparatus. The hydraulic jacks were connected in parallel and activated by a hand pump (700 bar). The testing apparatus was moved and rearranged for each test, so to avoid to move specimens and damage them. Each vault was built on two H shape steel beams, simulating the abutments, which were fixed to the concrete basement and bolted at ends to the contrast frame.

With the aim to reproduce as close as possible a distribution of the horizontal load proportional to the vault mass, both the actuators were connected to the vault through a pinned frame system composed of steel plates and pipes assembled by means of knuckle joints and calibrated pins. A sliding guide system provided the supports for the loading devices, permitting adaptation to the specimen deformation with negligible friction. Eight loading points were created at each side of the vault; the loading arms were fixed to the masonry by friction, tightening bolts placed at the lateral ends of steel plates applied along the masonry thickness.

The sixteen loading points were provided with loading cells (3 kN), to monitor the applied load. Moreover, the global load was measured through a pressure transducer. Potentiometer transducers, fixed on steel supports independent to the experimental apparatus, surveyed the vertical and the horizontal displacements of seven points, per each side of the vault. The measurement equipment was connected to an electronic acquisition unit interfaced with a computer, permitting a real-time monitoring of the loads-displacements story.

The tests were carried out imposing a cyclic variation of the horizontal load between two opposite values that were gradually increased during the test (step amplitude ±1 kN, rate ≈ 35 N/s) up to reaching the first cracking load. Then, the tests were prosecuted at displacement control, on the basis of the horizontal displacement monitored at the crown section (step amplitude ±10 mm, rate 0.5 mm/s).

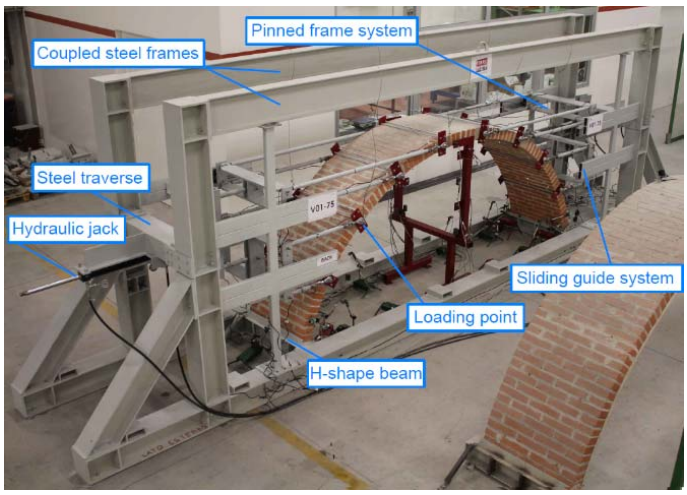

Figure 3. Illustration of the test setup

Test results. The results of the three tested samples are illustrated in Figure 4a, 5a and 6a in terms of F_h-δ_h curves, representing horizontal load against the horizontal displacement measured at the crown section. Schematizations of the crack patterns just before collapse, for both loading directions, are also reported: the thick symbols distinguish cracks in masonry, which induced the formation of a hinge, thinner labels indicate partial cracks which involved the mortar layer only. The diffusion of the cracks in the plaster is indicated with a jagged line.

In the unreinforced vault V01-75-NR (Figure 4a), the formation of the first crack ("N_A") emerged at the extrados near the right skewback, at about -1.5 kN, and caused a stiffness reduction. Similarly, a crack emerged at the extrados of the left skewback, at about +2.6 kN ("N_B"). Another crack formed at the extrados, in correspondence of a right haunch section ("N_C"), for a load of +3.7 kN. Then, in the next cycle, the suddenly opening of three cracks occurred at about -3.8 kN: one at the extrados, at left haunch ("N_D"), and the other two at intrados, at left skewback ("N_E") and at crown section ("N_F"). These three hinges, together with the hinge "N_A", determined the formation of the vault failure mechanism and the immediate collapse. The maximum horizontal displacement of the crown section reached just before the collapse was -0.8 mm. The position of the cracks is also schematized in the F_h-δ_h graph in Figure 4a. It is observed that the cracks developed almost entirely along a single mortar joint, mostly at the block-mortar interface (Figure 4b-c).

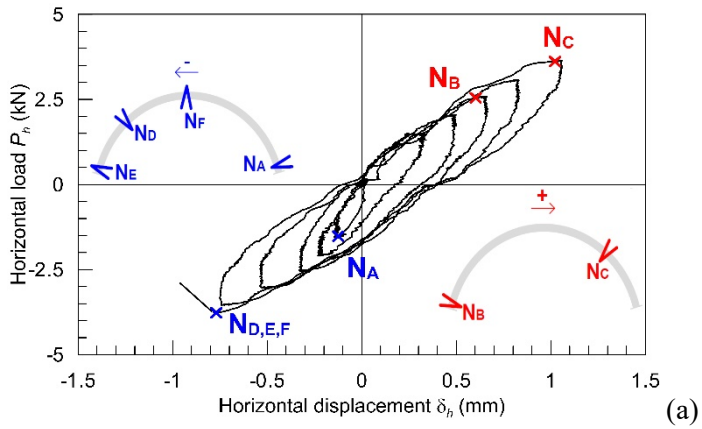

(a)

(b)

(c)

Figure 4. Sample V01-75-NR: (a) experimental P_h-δ_h curve with indication of the cracking section and detail of the opening of cracks (b) "N_D" and (c) "N_E" at the end of the test

In the vault strengthened at the extrados, V02-75-RE (Figure 5a), a first crack in the mortar layer, at the extrados of the right haunch, occurred at about +6.0 kN ("E_A"), without causing appreciable deviations from linearity of the load-displacement curve; similarly a crack in the mortar layer at the left haunch emerged at about -10.0 kN ("E_B"). Cracks then opened also at the intrados of the left ("E_C", at +10.0 kN) and right ("E_D", at -12.0 kN) haunches, inducing a visible stiffness reduction of the sample. At the increasing of the imposed displacement, cracks opened also in correspondence of the two skewbacks ("E_F" and "E_G", at $\delta_h \approx$ +10-15 mm, and "E_H" and "E_I", at $\delta_h \approx$ -10-15 mm). However, the sample collapse not yet occurred: in fact, the GFRP mesh across the cracks in the mortar layer ("E_A" and "E_B") opposed to the cracks opening and did not permit the formation of the hinge. Actually, at the increasing of the displacement, a sequence of additional cracks, almost equally spaced, formed in the mortar layer, at the haunches (Figure 5b). Moreover, the formation of 2-3 sequential intrados cracks in the masonry, at haunches, accompanied by the closing of the existing cracks in the vicinity (starting from "E_C" and "E_D"), was observed (Figure 5c). The load increases very little at each cycle, but a large increase of displacement was possible, due to the presence of the GFRP reinforcement embedded in the plaster. The maximum load attained -14.1 kN, in correspondence of a horizontal displacement at the crown section of -82.2 mm. Then, the rupture of the GFRP twisted wires occurred in correspondence of a haunch section, inducing the abrupt decrease of the resistance and the vault collapse (Figure 5b).

The first cracks in sample V03-75-RI, enhanced with GFRM at the intrados (Figure 6a), formed at about +11.0 kN: two at the extrados, at right haunch ("I_A") and at the left skewback ("I_B"), and the other one at intrados, at the left haunch ("I_C"). Similarly, at -11.0 kN, two cracks at the extrados, at left haunch ("I_D") and at the right skewback ("I_E"), and at intrados, at the right haunch ("I_G"), appeared; moreover, an intrados crack at left skewback ("I_F") occurred. At the increasing of the displacement, the cracks

diffusion was observed in the mortar layer, at the right haunch, since the GFRP mesh prevented the opening of crack "I_G" (Figure 6b). In the next loading cycle (at δ_h = -12 mm), a crack opened at the intrados, on the right skewback ("I_I"), and the cracks diffusion in the mortar layer was observed at the left haunch. The sequential formation of some other extrados cracks in masonry (2-3), in the vicinity "I_A" and "I_D", was observed (Figure 6c). The peak load reached -11.6 kN; the collapse was reached at about -9.5 kN (δ_h = -96.7 mm), when the GFRP twisted wires broke abruptly at the right haunch (Figure 6b). Actually, in the positive loading direction, an evident sliding occurred at one spring section (left) during the test, once a passing-through slot opened at the skewback, due to cyclic loading: this did not allow to exploit entirely the resistant contribution of the FRM layer, resulting in a lower post-cracking resistance. Differently, the sliding at the right spring section, for the negative direction, resulted quite restrained, thus an higher post-cracking load resulted.

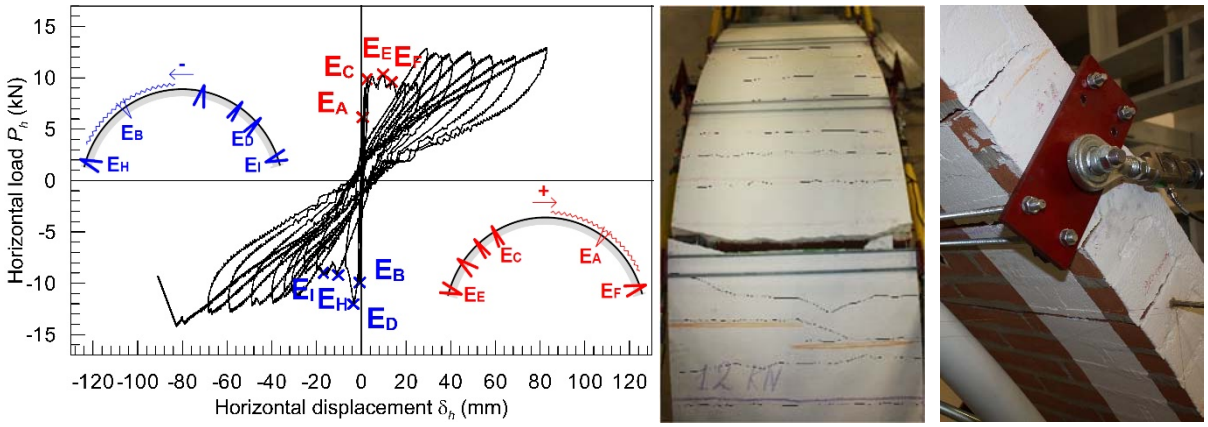

(a) (b) (c)

Figure 5. Sample V02-75-RE: (a) experimental P_h-δ_h curve, (b) top view of the mortar cracks and of the GFRP mesh failure of the left haunch, at collapse, and (c) detail of the sequential cracks formed in masonry, at right haunch

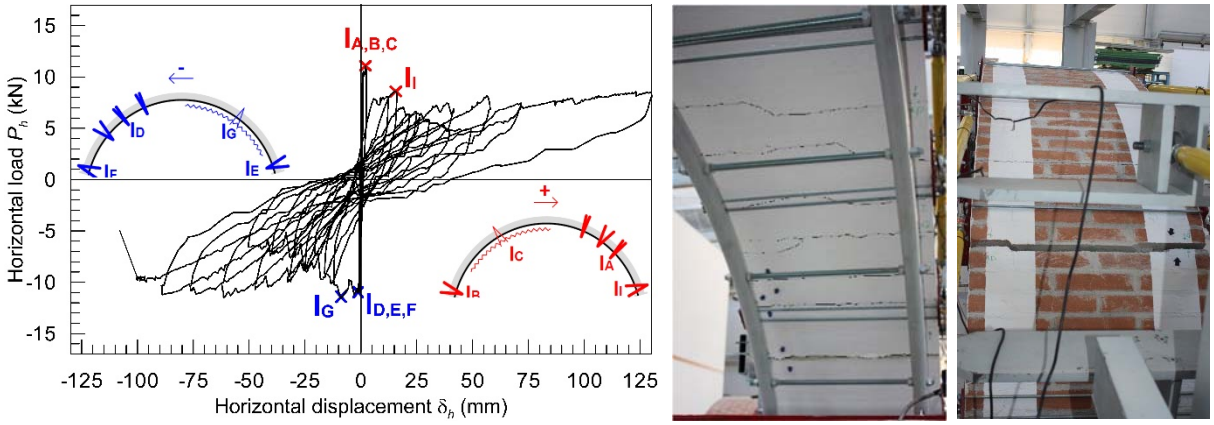

(a) (b) (c)

Figure 6. Sample V03-75-RI: (a) experimental P_h-δ_h curve, (b) bottom view of the mortar cracks of the right haunch, at collapse, and (c) detail of the sequential cracks formed in masonry, at left haunch

It is observed that in both tests on reinforced vaults some horizontal sliding occurred at the springer section when the cracks formed at skewback, so an additional device was added to stop this sliding, because in the vault in a building this displacement is not allowed due to the connection with the abutments.

A consistent resistance capacity increase emerged from the comparison of the results: the ultimate load was 3.8 times and 3.1 times that of the unreinforced vault, respectively, for V02-75-RE and V03-75-RI. Moreover, very large improvements in terms of displacement capacity were obtained: the ultimate horizontal displacements at crown section resulted, respectively,103 and 121 times greater than that of the unreinforced vault. The diffusion of parallel cracks emerged in the GFRM layers is in accordance with the typical behavior of reinforced elements subjected to tension, as was already observed both from tensile tests on GFRP reinforced mortar layers [16] and four point bending tests on GFRM reinforced masonry walls [10]. No detachment of the mortar layer was observed up to the collapse of the vaults.

3. Numerical simulations

The software Midas FEA (2016, ver 1.1) was utilized to simulate the behavior of the three masonry vaults tested experimentally (see section 2). In this first numerical simulation only monotonic loading was considered. The characteristics of the model, the numerical findings and the comparison with the experimental results are reported in the following.

Model characteristics. The numerical model is schematized in Figure 7a. A bi-dimensional model was adopted, so to simplify and accelerate the analysis; the influence of edge effect in the stress pattern was assumed negligible. A "smear-crack model" and a "total strain crack" criteria were assumed [17], with four-node plane strain elements employed for both the masonry and the mortar of the GFRM layers: the mesh dimension was about 1/10 and 1/3 of the global layer thickness, respectively; the mesh width was 60 mm. For plane elements, a nominal thickness of 66 mm was considered, that is the influence area of a single GFRP wire. The GFRP twisted wire was modelled by means of truss elements placed in the mortar thickness (mesh length 60 mm); the influence of the perpendicular GFRP wires was neglected. A fixed constraint was considered in correspondence of the skewbacks; however a horizontal linear spring (K = 10000 N/mm) was introduced, so to account for small adjustments of the vaults support system, monitored experimentally. However, these displacements resulted negligible for the reinforced samples. Pinned-nodes frames were introduced so to equally distribute the applied load among the eight loading points. The numerical simulations concerned nonlinear static analysis: at first, the vault self-weight acting in the vertical direction was applied, then the horizontal action was incremented step-by-step. The Newton-Rapshon iterative method was applied, with energy convergence criteria (percentage tolerance fixed to 10^{-3}).

The materials were considered homogeneous and isotropic. The specific weights were 18 kN/m^3, for the masonry and 20 kN/m^3 for the mortar of the reinforcement. The mechanical characteristics of the masonry referred to previous experimental investigations carried out by the authors, concerning compressive tests and out-of-plane four point bending tests on solid brick masonry [10]: in particular, an elastic-plastic behavior in compression, with Young modulus E_m = 5054 MPa and strength $f_{c,m}$ = 9.3 MPa was considered; in tension, an elastic-brittle behavior, with strength $f_{t,m}$ = 0.4 MPa (flexural tensile strength with respect to an axis parallel to bed joints) was adopted. The Poisson ratio was assumed equal to 0.25. The perfect adhesion between the coating and the masonry was assumed, as no slip emerged in experimental tests. The Young modulus and compressive resistances of the mortar were those obtained from the experimental characterization tests (see section 2). An elastic-plastic behavior in compression (ultimate strain $\varepsilon_{u,c}$ = 3.5 $^0/_{00}$) and a Poisson ratio υ = 0.2 were considered. An elastic-brittle behavior was assigned to the GFRP wire (stiffness and tensile limit according to Table 1). The tension stiffening of the mortar between cracks was taken into account by modifying the mortar softening relationship so to fit the experimental test results on reinforced mortar layers (Figure 2b). In particular, the tensile stress-strain curve considered for the mortar was drown in Figure 2b, as difference between the global behavior of the reinforced mortar coating and that of the GFRP wire. The ultimate displacement of the reinforced mortar coating corresponded to the load related to the wires rupture.

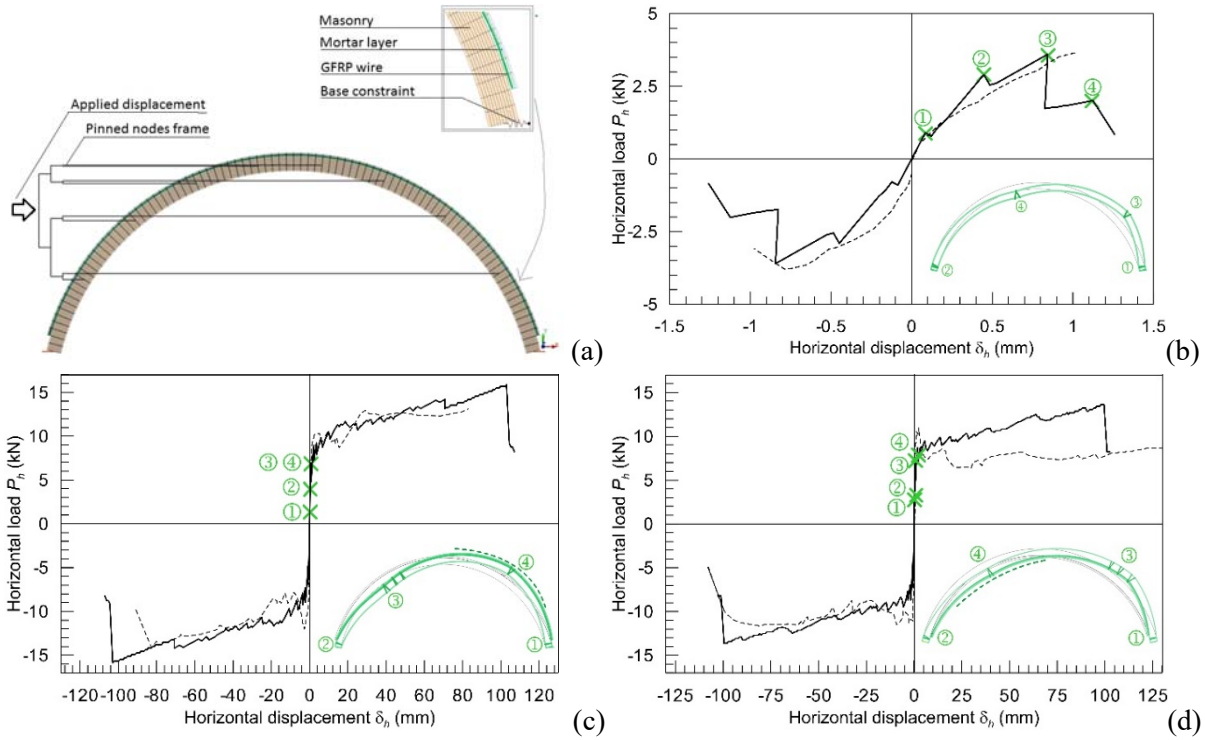

Figure 7. Numerical simulations: (a) schematization of the numerical model and comparison between numerical and experimental capacity curves of vaults (a) V01-75-NR, (b) V02-75-RE and (c) V03-75-RI

Numerical results and discussion. In the numerical modelling of the unreinforced vault (Figure 7b) an initial linear elastic behavior emerged; then, the sequential opening of four cracks in correspondence of the skewbacks and of the haunches occurred, as the masonry tensile resistance at intrados or extrados was exceeded. The formation of the four hinges (according to the sequence indicated in Figure 7b) induced the vault collapse. The numerical capacity curve is compared with both branches (positive and negative) of the experimental backbone curve: a good accordance of the results emerged, both in terms of resistance and displacement capacities.

The simulation of the vault reinforced at extrados (Figure 7c) evidenced an initial linear stiffness higher than that of the unreinforced one, due to the thicker cross section and the higher Young modulus of the mortar of the coating, in respect to that of masonry. At first, sequential cracks occurred at the spring sections (the former at intrados, the latter at extrados); then, a crack formed at the tensed intrados of a haunch, when the masonry tensile strength was attained, inducing the formation of the third hinge. The tensile resistance of the mortar was attained at the tensed extrados of the other haunch, but the GFRP wires prevented the crack opening and the formation of another hinge. Very large horizontal displacements at keystone section were attained. As the displacement δ_h increased, the formation of new hinges, at the intrados of an haunch, occurred in the masonry, below the first one. The collapse of the vault occurred in consequence of the tensile rupture of the GFRP wires at the opposite haunch. A diffusion of the plasticization in a wider area of mortar layer emerged. Actually, the numerical capacity curve attained to higher values of both resistance and ultimate displacement; however, the trend of both branches of the experimental backbone curve was reproduced with quite accuracy by the numerical model. Small differences in the GFRP wires tensile strength and in the positioning of the mesh inside the mortar thickness could have anticipated the collapse. Moreover the progressive damage accumulated during cycles causes a lower envelope curve with respect to the monotonic one. Such a damage is however quite limited.

Similarly, the cracks formation in the vault reinforced at intrados (Figure 7d) started from the skewbacks, then extended at one haunch, where the masonry cracks at the tensed side (extrados), and affected the mortar coating (at the intrados of the other haunch). A diffuse plasticization occurred in the reinforced mortar coating at the increasing of δ_h. New hinges formed in masonry at the extrados of a haunch, in the vicinity of the first one. The collapse of the vault occurred in consequence of the tensile rupture of the GFRP wires at the opposite haunch, at intrados. It is observed that the numerical capacity curve fitted quite well the trend obtained experimentally, when the negative loading direction is considered. Differently, the experimental values of the post-cracking load resulted lower than the numerical prediction; in fact, as already evidenced in section 2, an evident sliding at one spring section, in the positive loading direction, emerged during the test.

In general, it can be observed that the simplified numerical simulations, based on a bi-dimensional model and on a monotonic, nonlinear static analysis, are able to reproduce with quite good accuracy the experimental performances of both unreinforced and reinforced vaults.

4. Conclusions

The paper investigates on a modern strengthening technique for masonry vaults consisting in the application of a reinforcement made of glass fibre reinforced polymer (GFRP) meshes embedded in a thin mortar coating (about 30 mm) anchored to the masonry vault by means of GFRP connectors. In particular, the results of a first set of experimental tests carried out of full-scale masonry vaults (thickness 120 mm, arch span 4000 mm, arch rise/radius = 0.75), subjected to horizontal quasi-static cyclic loading, so to check the effectiveness of the strengthening technique on masonry vaults were summarized and the reliability of a simplified numerical model developed by the authors to simulate the vaults behavior was checked. A particular attention was devoted to the design of the experimental test setup, able to reproduce the effect of a horizontal load distributed proportionally to the vault mass and acting cyclically, in the vault transversal direction. In fact, a previous numerical study presented by the authors evidenced that simplified loading patterns commonly adopted in the literature for experimental investigations, based on concentrated loads, are not suitable for the evaluation of the actual behavior of reinforced vaults.

The results of three tests on masonry vaults were presented and compared: one unreinforced and the other two strengthened using the considered GFRM technique applied at the extrados or at the intrados. The results evidenced the excellent performances attributable to the reinforcement application: a resistance increase ranging from 3.1 to 3.8 and a displacement capacity close to one hundred times greater than that of the unreinforced one were obtained. In particular, it is worth note that the high ductility obtained is due to the presence of the GFRP reinforcement embedded in the mortar layer, which guarantees a significant resisting moment once the mortar cracks.

The behavior of the three experimental sample was then simulated numerically, using a simplified bi-dimensional smear-crack model based on monotonic, nonlinear static analysis. The characteristics of the materials were derived from experimental characterization tests. The experimental and numerical results were compared in terms of capacity curves expressing the global horizontal load against the horizontal displacement at the crown section. Though the analysis were based on a monotonic loading, a good accordance between experimental and numerical findings emerged.

In general, test results provided very useful and original information on the effectiveness of the reinforcement technique, highlighting also some important aspects, such as the correct design of the connection of the reinforcement to the abutment, which will be taken into account in the continuation of the study. Other three specimens, with a different rise/radius ratio (0.5), are going to be tested, so to enlarge the experimental database and extend the validity of the numerical predictions. Moreover, a

more detailed numerical model, accounting for the effect of cyclic loading in the material degrade is in progress, so to provide more refined results.

Acknowledgments
This paper is based on part of a research project financed by the composite engineering factory FibreNet s.r.l., Pavia di Udine, Italy. The financial support of "Reluis 2017" is gratefully acknowledged. The authors wish also to thank Allen Dudine, Enrico Zanello, Davide Menegon, Norman Bello, Alessandra Gubana and Carlos Passerino for the useful help provided during the tests.

References
[1] M.R. Valluzzi, M. Valdemarca, and C. Modena, "Behavior of Brick Masonry Vaults Strengthened by FRP Laminates", *J. of Comp. for Cons.*, vol. 5, issue 3, pp. 163-169, 2001.
[2] P. Foraboschi, "Strength assessment of masonry arch retrofitted using composite reinforcements", *Masonry International*, vol. 15, issue 1, pp. 17–25, 2001.
[3] D. Oliveira, I. Basilio, and P. Lourenço, "Experimental Behavior of FRP Strengthened Masonry Arches", *Journal of Composites for Construction*, vol. 14, issue 3, pp. 312-322, 2010.
[4] A. Borri, P. Casadei, G. Castori, and J. Hammond, "Strengthening of Brick Masonry Arches with Externally Bonded Steel Reinforced Composites", *Journal of Composites for Construction*, vol. 13 , issue 6, pp. 468-475, 2009.
[5] L. Bednarz, A. Gorski, J. Jasienko, and E. Rusinsk, "Simulations and analyses of arched brick structures", *Automation in Construction*, vol. 20, pp. 741–754, 2011.
[6] L. Hojdys, and P. Krajewski, "Experimental tests on strengthened and unstrengthened masonry vault with backfill", *Journal of Heritage Conservation*, vol. 32, pp. 105-108, 2012.
[7] P. Girardello, F. Da Porto, C. Modena, and M.R. Valluzzi, "Experimental behavior of masonry vaults reinforced with composite materials in inorganic matrix" (in Italian), *2013 ANIDIS XV Conf. Seismic Engineering in Italy*, Padua, 30th June - 4th July.
[8] L. Garmendia, P. Larrinaga, R. San-Mateos, and J.T. San-José, "Strengthening masonry vaults with organic and inorganic composites: an experimental approach", *Materials and Design*, vol. 85, pp. 102–114, 2015.
[9] N. Gattesco, and I. Boem, "Experimental and analytical study to evaluate the effectiveness of an in-plane reinforcement for masonry walls using GFRP meshes", *Const and Build. Mat.*, vol. 88, pp. 94-104, 2015.
[10] N. Gattesco, and I. Boem, "Out-of-plane behavior of reinforced masonry walls: Experimental and numerical study", *Composites Part B*, vol. 128, pp- 39-52, 2017.
[11] N. Gattesco, and I. Boem, "Strengthening of masonry vaults through a thin extradoxal layer of fiber reinforced lime mortar", *2016 SAHC, Proc. of the 10th Int. Conf. on Structural Analysis of Historical Constructions*, Leuven, 13-15 September.
[12] EN 772-1:2011+A1:2015, "Methods of test for masonry units - Part 1: Determination of compressive strength".
[13] EN 12390-3:2009/AC:2011, "Testing hardened concrete - Part 3: Compressive strength of test specimens", CEN, Brussels.
[14] EN 12390-6:2009, "Testing hardened concrete - Part 6: Tensile splitting strength of test specimens", CEN, Brussels.
[15] EN 12390-13:2013, "Testing hardened concrete - Part 13: Determination of secant modulus of elasticity in compression", CEN, Brussels.
[16] N. Gattesco, and I. Boem, "Characterization tests of GFRM coating as a strengthening technique for masonry buildings", *Composite Structures*, vol. 165, pp. 209-222 , 2017.
[17] TNO Building and Construction Research. *DIANA – Finite Element Analysis User's Manual*. Release 8.1 September 2002.